Stresses in Laser-Beam-Welded Lap Joints Determined by Outer Surface Strains

Attaching two or three strain gauges to the outer surface of overlap sheets near the joint can be used as a strain gauge method for determining inaccessible stresses

BY S. ZHANG

ABSTRACT. Fatigue strength of laser-beam-welded lap joints is usually assessed on the basis of structural stresses in the joints. Stresses are nevertheless difficult to determine due to overlap of welded sheets. This article describes a strain gauge method that can determine inaccessible stresses by attaching two or three strain gauges to the outer surface of the overlap sheets near the joint. The method is validated by finite element simulations. Results obtained from the current method are compared with those from the literature.

Introduction

Laser beam welding of thin sheet metals has been increasingly applied in the automotive and other industries. Lap joints are one common structural design. The lap joint subjected to tensile shear (Fig. 1) is a critical loading condition. The fatigue strength of such joints has been widely analyzed and measured (Refs. 1–9) based on structural stresses at the weld root in the joint. References 1–6 correlated fatigue test results across different weld sizes or different sheet thickness combinations by using empirical stress parameters or structural stresses. In the latter case, there is still no reliable measuring method for determination of structural stresses in the weld or at the weld root. Fracture mechanics parameters such as stress intensity factors, notch stress, and energy release rate were also tried in correlation with fatigue test data. They showed no better results than structural stresses (Ref. 9). Some test data appear to be contaminated by experimental uncertainties due to a lack of measuring methods capable of direct determination of the strength-decisive stresses at the weld. The difficulty in developing such a measuring method is attributable to poor accessibility to the weld root resulting from sheet overlap.

This paper describes a method capable of determining inaccessible stresses by measuring the outer surface strains in the neighborhood of the joint. The method is validated by finite element simulations and applied to a tensile shear specimen considered in the literature.

S. ZHANG (shicheng.zhang@daimlerchrysler.com) *is with Research and Technology, Daimler Chrysler AG, Stuttgart, Germany.*

KEY WORDS

Fatigue Strength
Lap Joint
Laser Beam Weld
Strain Gauge
Struetural Stress

Analysis

The stress state in a lap joint is normally considered by a strip model (Fig. 1). The strength-relevant stresses are shear stress τ_w (considered as mean stress here) in the weld at the interface of the two joined sheets and normal stress σ_{si} on the inner side of the sheet at the weld root. These stresses are regarded as structural stresses. Plasticity and residual stresses are not considered. Forces and stresses in seam-welded lap joints, including laser welds, were considered in Ref. 7. A strain gauge solution was developed where forces and stresses in a lap joint could be determined by several strain gauges attached only to the outer surface of the joined sheets. The solution was based on elementary plate theory and equilibrium conditions. The fundamental formulas of the strain gauge solution were also found in Ref. 8.

Based on published formulas, the general solution was further worked out to obtain a special solution for the laser-welded lap joint. A strain gauge method was then obtained that enabled the inaccessible stresses at the weld root to he determined by three strain gauges attached only to the outer surface of the lap joint. The method is based on the strain gauge configuration shown in Fig. 2.

The place where the strain gauges are attached is referred to as the measuring position. Note the measuring position is not the position where stresses σ_{si} and τ_w are. Strains ε_{uo} and ε_{lo} were determined by two outer surface strain gauges. Stresses σ_{uo} and σ_{lo} at the measuring position (Fig. 3) were determined by Hooke's law, *i.e.*, $\sigma_{uo} = E'_u\varepsilon_{uo}$ and $\sigma_{lo} = E'_l\varepsilon_{lo}$. Another strain gauge ε_{uo2} (the subscript 2 indicates the second strain gauge adjacent to ε_{uo}) was added to determine strain gradient ε'_{uo}.

The strain gradient was calculated by $\varepsilon'_{uo} = \Delta\varepsilon/\Delta x = (\varepsilon_{uo2}-\varepsilon_{uo})/\Delta x$ with $\Delta x > 0$ being the distance of the two neighboring strain gauges. To ensure the accuracy of the strain gradient, Δx was kept small. According to elementary plate theory, the transverse shear stress τ_{qu} in the upper sheet at the measuring position (Fig. 3) was determined in mean value as follows:

$$\tau_{qu} = \frac{t_u}{6} E'_u \varepsilon'_{uo} \qquad (1)$$

The lower sheet was determined by force equilibrium condition in the y direction, *i.e.*, $\tau_{ql}t_l = \tau_{qu}t_u$.

The parameter E'_j(j = u, l) was de-

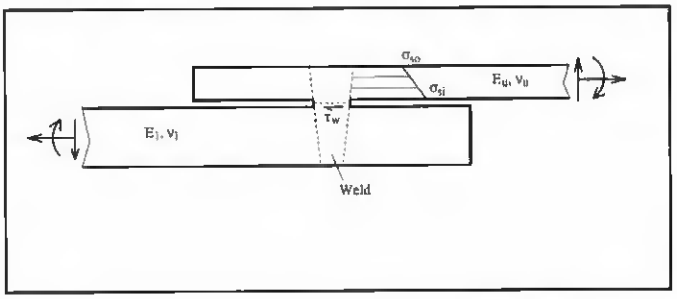

Fig. 1 — Laser-welded lap joint and structural stresses in the joint.

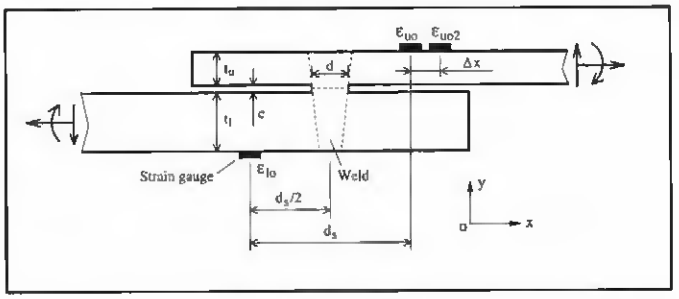

Fig. 2 — Strain gauge configuration for determining inside structural stresses.

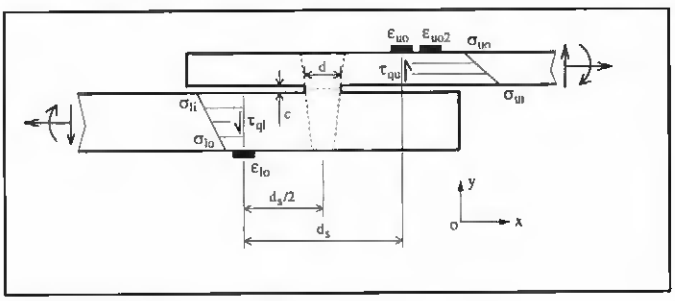

Fig. 3 — Stresses at measuring position.

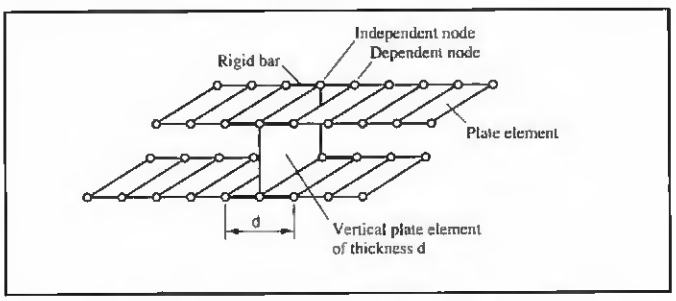

Fig. 4 — Finite element model in principle for laser welded lap joint.

fined $E'_j = E_j$ for conditions of plane stress and $E'_j = E'_j/(1-\nu_j^2)$ for conditions of plane strain in the z direction. Young's modulus E_u, Poisson's ratio ν_u, and thickness t_u refer to the upper sheet, and E_j, ν_j, and t_l to the lower one. Without loss in generality, $t_l \geq t_u$ is assumed. Parameters d, d_s, and c indicate weld widths at the interface, spacing of the strain gauges, and gap width between the two overlap sheets (Fig. 2), respectively.

To ensure application of elementary plate theory, the condition $d_s \geq 2t_l + d$ should be met (Refs. 7 and 8). The two neighboring strain gauges ε_{uo} and ε_{uo2} were attached to the thinner sheet.

Based on the above, the real unknowns for complete determination of the stress state at the measuring position were the two inaccessible stresses σ_{ui} and σ_{li} on the inside of the overlap sheets. However, the two unknowns could be determined by two other equilibrium conditions (force and moment in x-direction). So all stresses at the measuring position were determined either by direct strain measurement or by application of equilibrium conditions.

As long as the complete stress state at the measuring position has been determined, stresses at the weld can be derived simply by shifting the stresses at the measuring position to the weld aided by equilibrium conditions. The following formulas can then be derived for the two strength-relevant stresses in the joint under tensile-shear loading condition:

$$\sigma_{si} = \frac{1}{t_u\left(t_u + t_l + 3c\right)} \left[\begin{matrix} t_u^2 d_s E'_u \varepsilon'_{uo} - t_u\left(2t_u + t_l + 3c\right) \\ E'_u \varepsilon_{uo} - t_l^2 E'_l \varepsilon'_{lo} \end{matrix} \right] + \frac{1}{2}\left(d_s - d\right) E'_u \varepsilon'_{uo}, \quad (2)$$

$$\tau_w = \frac{1}{2d\left(t_u + t_l + 3c\right)} \left(\begin{matrix} t_u^2 d_s E'_u \varepsilon'_{uo} - t_u^2 d_s E'_u \varepsilon_{uo} \\ - t_l^2 E'_l \varepsilon_{lo} \end{matrix} \right) \quad (3)$$

Equations 2 and 3 show the stresses in the weld are actually determined by three outer surface strain gauges. The sign convention of normal strains/stresses (positive for tensile and negative for compressive) has been taken into account in the two equations. The positive sign of the shear stresses is given in Figs. 1 and 3. The bending effect of τ_{qu} and τ_{ql} relative to the weld root have also been included in the two equations.

The stress state at a weld root is multiaxial and so an equivalent stress is required. The following von Mises equivalent stress was proposed in Ref. 5 by combining the normal stress at the weld root with the mean shear stress in the weld:

$$\sigma_{eq} = \sqrt{\sigma_{si}^2 + 3\tau_w^2} \quad (4)$$

The problem with the above equation is the two stresses do not occur at the same location, which contradicts the definition of von Mises' stress.

New solutions for stress intensity factors, notch stress, and J integral have recently become available for spot welds (Refs. 10 and 11) and have been successfully applied to correlating fatigue strength across different specimens and different weld geometries (Refs. 12 and 13).

These solutions are also suited for recovering stress intensity factors and notch stress at spot welds in finite element analysis (Refs. 14 and 15). The relation between notch and structural stress is approximately applied here to laser welds. Based on the results of Refs. 10–12, the following equivalent stress is proposed:

$$\sigma_{eqk} = \frac{2\delta\sigma_{so} + \delta\left(2 - \delta + \delta^2\right)\sigma_{si}}{\left(1+\delta\right)^3} + C_o\left[C_1/C_2 \pm \sqrt{\left(1+3\delta^2\right)\sigma_{ui}^2 + \sigma_{so}^2 + \left(1-3\delta\right)\sigma_{si}\sigma_{so}}\right] \quad (5)$$

Table 1 — Angular Function ϖ (δ) (Ref. 16)

$\delta = t_u/t_l$	1.0	0.5	0.1	0.0
ϖ in degrees	49.1	49.8	54.6	52.1

Table 2 — Comparison between Results of Finite Element Simulation and Present Method

		σ_{si}		τ_w	
		FEM	Equation 2	FEM	Equation 3
0.9/0.9,	$c = 0$	281.1	279.4	62.2	63.9
0.9/2.0,	$c = 0$	278.2	275.2	62.3	64.3
2.0/2.0,	$c = 0$	127.0	126.9	62.5	64.5
0.9/0.9,	$c = 0.2$	330.0	328.6	63.1	64.5
0.9/2.0,	$c = 0.2$	308.5	304.9	62.8	64.5
2.0/2.0,	$c = 0.2$	136.8	136.7	62.7	64.7

*Homogenous materials with $E_u = E_l = 2.1 \times 10^5$ MPa and $\nu_u = \nu_l = 0.3$; different sheet thickness combinations (0.9/0.9, 0.9/0.2, and 2.0/2.0), without and with a root opening between the overlap sheets ($c = 0$ and 0.2 mm); and under tensile-shear force of $F = 2$ kN.

Table 3 — Comparison between Results of Finite Element Simulation and Present Method

		σ_{si}		τ_w	
		FEM	Equation 2	FEM	Equation 3
0.9/0.9,	c = 0	307.6	306.8	61.7	63.2
0.9/2.0,	c = 0	354.4	350.4	62.6	64.0
2.0/2.0,	c = 0	137.8	138.2	62.4	64.1
0.9/0.9,	c = 0.2	364.1	364.9	62.6	64.1
0.9/2.0,	c = 0.2	394.8	390.8	63.0	64.3
2.0/2.0,	c = 0.2	148.6	149.4	62.6	64.5

*Dissimilar materials with $E_u = 3E_l = 2.1 \times 10^5$ MPa and $\nu_u = 0.3$, $\nu_l = 0.28$; different sheet thickness combinations (0.9/0.9, 0.9/0.2, and 2.0/2.0), without and with a root opening between the overlap sheets ($c = 0$ and 0.2 mm); and under tensile-shear force of $F = 2$ kN.

$$C_o = \frac{\sqrt{t_u/\rho}}{\sqrt{6\pi\left(1+\delta\right)^3}} \qquad (6)$$

$$C_1 = \begin{bmatrix}\left(1+3\delta+6\delta^2\right)\tan\omega \\ -\sqrt{3}\left(1+\delta\right)\end{bmatrix}_c - \left[\left(1+3\delta\right)\tan\omega + \sqrt{3}\left(1+\delta\right)\right]_{c'}$$

$$C_2 = 2\sqrt{(1+3\delta+3\delta^2)(1+\tan^2\omega)} \qquad (8)$$

with $\delta = t_u/t_l$ and ρ notch root radius at the weld. The angular parameter ω depends on δ and is quoted as Table 1 from Ref. 16. The combined sign "±" in Equation 5 takes the plus if $[(1+3\delta+6\delta^2)\tan\omega - \sqrt{3}(1+\delta)]\sigma_{si} - [(1+3\delta)\tan\omega + \sqrt{3}(1+\delta)]\sigma_{so} \geq 0$ and otherwise the minus. The above equivalent stress is actually T-stress (non-singular stress) plus notch stress at the weld root. In other words, Equation 5 is the maximum tangential stress along the interior surface of the weld root. The weld root radius ρ is difficult to determine in practice, so a fictitious rounding concept (Ref. 17) was used to help overcome this difficulty. The concept enables an unambiguous notch root radius to be defined for a given material and ρ = 0.1–0.2 mm can be introduced for common ferritic steels (Ref. 17). An outer surface stress σ_{so} is additionally needed in Equation 5 and is determined by the equation

$$\sigma_{so} = \frac{E'_u}{2}\left[2\varepsilon_{uo} - \left(d_s - d\right)\varepsilon'_{uo}\right] \qquad (9)$$

In comparison to Equation 4, Equation 5 captures the complete stress state at the weld since both inner and outer surface stresses are included in the formula. Sheet thickness, thickness ratio of the two sheets, and notch root radius at the weld are additionally taken into account in Equation 5. This equivalent stress better reflects the local loading condition of the lap joint and is superior to Equation 4.

Another advantage of Equation 5 is that the equivalent stress can be either positive or negative, corresponding to a tensile or compressive stress state, which is especially important for cyclic loads. Equation 4, however, is always positive and makes no distinction between tensile and compressive stress states. The only disadvantage of Equation 5 is that it is much more complex than Equation 4.

In the case of equal sheet thickness, the above equations are simplified as follows:

$$\sigma_{si} = \frac{E'}{2}\left\{\left[\frac{d_s\left(4t+3c\right)}{2t+3c} - d\right]\varepsilon' - \frac{2\left(4t+3c\right)}{\quad}_{c}\right.$$

$$\sigma_{so} = \frac{E'}{2}\left[2\varepsilon_{uo} - \left(d_s - d\right)\varepsilon_{uo}\right] \qquad (11)$$

$$\tau_w = \frac{E't^2}{2d\left(2t+3c\right)}\left(d_s\varepsilon'_{uo} - 2\varepsilon_{uo}\right) \qquad (12)$$

$$\sigma_{eqk} = \frac{\sigma_{si}+\sigma_{so}}{4} + \frac{1}{4\sqrt{3\pi}}\sqrt{\frac{t}{\rho}}\left[\sigma_{si} - \sigma_{so} \pm \sqrt{3\sigma_{si}^2 + (\sigma_{si} - \sigma_{so})^2}\right] \qquad (13)$$

with $E'_u = E'_l = E'$, $\nu_u = \nu_l = \nu$, and $t_u = t_l = t$. The combined sign "±" in Equation 13 takes the plus if $\sigma_{si} - \sigma_{so} \geq 0$. If it does not, it will take the minus. In this case, the strain gauge on the other side (ε_{lo}) becomes redundant and all the stresses are then determined by only two strain gauges (ε_{uo} and ε_{ou2}) on one side of the specimen. This further simplifies experiments.

Validatinn of the Method

A direct experimental validation of the current method was impossible since there is no measuring method capable of determining the inside stresses. Instead, finite element simulations were conducted to validate the strain gauge method.

The finite element model for a laser lap joint is shown in principle in Fig. 4. Both the welded sheets and the weld were modeled by plate elements with a special connection through rigid bars that created weld width. Accordingly, the vertical plate element simulating the weld had a thickness of weld width. The element width in the region adjacent to the weld (rigid bars) had to be 0.3 mm in the present model to obtain reliable stresses and strains.

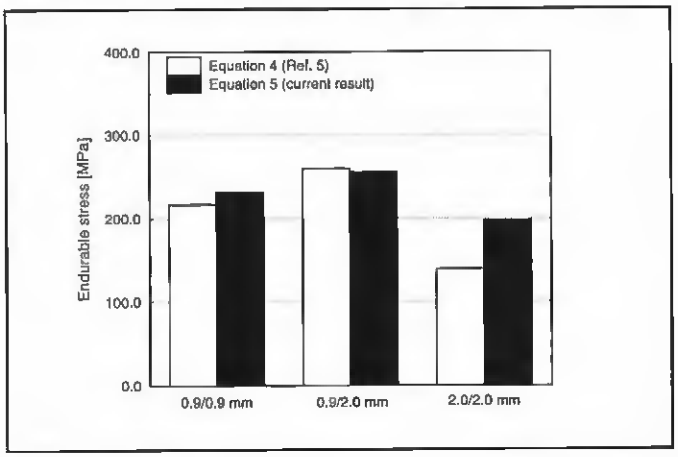

Fig. 5 — Comparison of endurable stress across three thickness combinations.

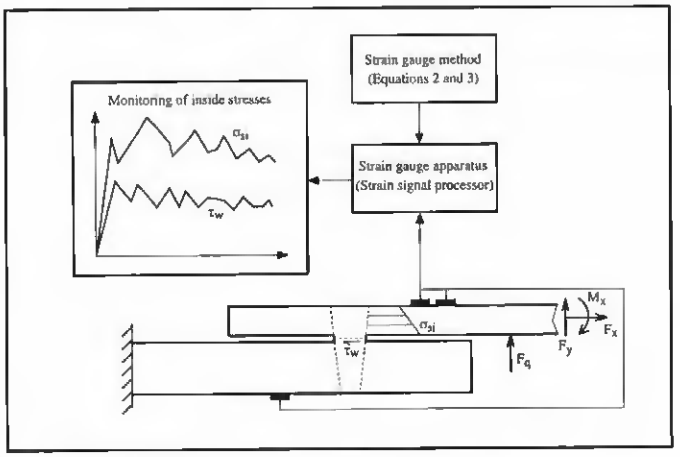

Fig. 6 — Monitoring of inside stresses in laser lap joints.

Simulations were based on a tensile-shear specimen considered in Ref. 5. The length, width, and overlap length of the specimen were 80, 32, and 32 mm, respectively. Two sheet thicknesses — t_u = 0.9 mm and t_l = 2.0 mm — generated three sheet thickness combinations of t_u/t_l = 0.9/0.9, 0.9/2.0, and 2.0/2.0.

The weld width, spacing of the strain gauges, and distance of the two neighboring strain gauges were d = 1.0, d_s = 7.3, and Δ_x = 0.3 mm, respectively. The two sheets were made of the same material with Young's modulus E_u = 210,000 MPa and Poisson's ratio v_u = 0.3, or of dissimilar materials with E_u = 210,000 MPa, E_l = 70,000 MPa, v_u = 0.3, and v_l = 0.28.

The strain gauges were assumed on the longitudinal central line of the specimen and the plane strain condition was introduced. To simulate real experiments, the specimen was loaded in the longitudinal direction without rotation at the two loading ends.

In the first run, stresses σ_{si} and τ_w were directly calculated (Tables 2 and 3, the values under FEM). These values were regarded as the real structural stresses in the joint. That was followed by the second run where the strains ε_{uo} and ε_{lo} and the strain gradient ε'_{uo} were calculated as if they were measured by the strain gauges. The same stresses σ_{si} and τ_w were predicted, this time by the strain gauge method, substituting the strains and the strain gradient into Equations 2 and 3 (Tables 2 and 3, the values under Equations 2 and 3). In this way, the stresses predicted by the strain gauge method can be checked by the values directly calculated by FEM. The check was made systematically for different sheet thicknesses and material combinations with or without a root opening between the overlap sheets (root opening width c = 0 or 0.2 mm). As seen from Tables 2 and 3, the stresses predicted by the strain gauge method were very close to the FEM results. The method was validated by the finite element simulations.

Another check of fatigue strength for the tensile-shear specimen (Ref. 5) was made. The measured strains (stresses) outside the overlap region were linearly extrapolated to the weld root to get the structural stresses and the equivalent stress (Equation 4) there. The endurable equivalent stress of Equation 4 was then determined in Ref. 5 by an extrapolation procedure at the endurable load. If the overlap length is found to be large in comparison to sheet thickness, as may be the case in practice, the accuracy of the extrapolated stresses at the weld root may be undermined by a large extrapolation range.

The newly introduced equivalent stress of Equation 5 with ρ = 0.1 mm was thus evaluated in finite element simulations. The endurable equivalent stress (fatigue strength) of Equation 4 (Ref. 5) and Equation 5 were compared in Fig. 5 for all three sheet thickness combinations. As can be seen from the figure, there were some deviations between the two endurable stresses. This is understandable because Equations 4 and 5 have different backgrounds. By comparing the endurable stress across the three thickness combinations, it became clear the endurable stress of Equation 5 showed a smaller deviation, indicating a better transferability of fatigue strength across the three thickness combinations. The results of Ref. 5 show a larger deviation, which may result from the superposition of the stresses at different locations (Equation 4) or from the extrapolation procedure.

The present strain gauge method is sketched in Fig. 6 to help establish a procedure to monitor the inside stresses in the joint. If Equations 2 and 3 are implemented in a strain signal processor, strain signals from the three strain gauges can easily be converted into inside stress signals. The inaccessible inside stresses can then be monitored by the strain gauges in real time or against applied loads. Note that all loads outside spacing d_s of the strain gauges, *e.g.*, an arbitrary force F_q (Fig. 6) or other excitations besides applied loads F_x, F_y, and M_x, were captured by the three strain gauges in terms of their contribution to the inside stresses.

Conclusion

A novel method was developed to enable the unaccessible, fatigue-relevant stresses in laser-welded lap joints to be determined by two or three strain gauges attached only to the outer surface of the joined sheets near the weld. The method was validated by finite element simulations that assumed the welded sheets behave in accordance with the elementary plate theory. This implies the strain gauges should be spaced at appropriate intervals from the weld ($d_s \geq 2t_l + d$). (Plasticity and residual stress were not considered and the method has not yet been applied to real experiments.)

When applying the method, it is important to accurately measure geometric parameters such as weld width d, root opening width c, spacing d_s of the strain gauges, and distance Δ_x of the two neighboring strain gauges. The newly proposed equivalent stress σ_{eqk} may be considered as an alternative to Equation 4 since it better correlates fatigue test results. The complexity of the formula for σ_{eqk} is, however, an obvious disadvantage.

References

1. Hsu, C., and Albright, C. E. 1991. Fatigue analysis of laser welded lap joints. *Engi-*

neering Fracture Mechanics 39: 575–580.

2. Wang, P. C. 1995. Fracture mechanics parameter for the fatigue resistance of laser welds. *International Journal of Fatigue* 17: 25–34.

3. Wang, P. C., and Ewing, K. M. 1994. Effect of weld design on the fatigue strength of laser and resistance spot-welded tubular T-joints for automotive applications. *Welding Journal* 73(9): 209-s to 217-s.

4. Wang, P. C., and Ewing, K. M. 1991. A comparison of fatigue strengths: laser beam vs. resistance spot welds. *Welding Journal* 70(10): 43-s to 47-s.

5. Sonsino, C. M., Müller, E., and Radaj, D. 1994. Ertragbare Strukturspannungen von lasergesehweißten Stahlbleehen. DVM-Bericht 120 "Fügen im Leichtbau." DVM, Berlin, 63–86.

6. Flavenot, J. E, Deville, J. P., Diboine, A., Cantello, M., and Gobbi, S. L. 1993. Fatigue resistance of laser welded lap joints of steel sheets. *Welding in the World* 31: 358-361.

7. Zhang, S. 1995. Forces and stresses in seam welded overlap joints. Research Report 95-0005. Stuttgart, Germany, Daimler-Benz AG.

8. Zhang, S., and Radaj, D. 1996. Forees and stresses in seam welded overlap joints derived from outer surface deformation. *Engineering Fracture Mechanics* 54: 743–750.

9. Radaj, D, Sonsino, C. M., and Zhang, S. 1999. Schwingfestigkeit laserstrahlgeschweißter Dünnblechproben aus Stahl nach lokalen Konzepten. *Materialwissenschaft und Werkstofftechnik* 30: 249–256.

10. Zhang, S. 1997. Stress intensities at spot welds. *International Journal of Fracture* 88:167–185.

11. Zhang, S. 1999. Stress intensities derived from stresses around a spot weld. *International Journal of Fracture* 99: 239–257.

12. Zhang, S. 1999. Approximate stress intensity factors and notch stresses for common spot-welded specimens. *Welding Journal* 78(5): 173-s to 179-s.

13. Zhang, S. 2001. Approximate stress formulas for a multiaxial spot weld specimen. *Welding Journal* 80(8): 201-s to 203-s.

14. Zhang, S. 1999. Recovery of notch stress and stress intensity factors in finite element modeling of spot welds. Proceedings of NAFEMS World Congress '99 on Effective Engineering Analysis, Newport, R.I., pp. 1103–1144.

15. Zhang, S. 2001. Recent developments in analysis and testing of spot welds. SAE Paper 2001-01-0432.

16. Suo, Z., and Hutchinson, J. W. 1990. Interface crack between two elastic layers. *International Journal of Fracture* 43:1–18.

17. Neuber, H. 1968. Über die Bertücksichtigung der Spannungskonzentration bei Festigkeitsberechnungen. *Konstruktion* 20: 245–251.

Call for Papers

The International Welding/Joining Conference, "Intelligent Technology in Welding and Joining," will be held October 28–30, in Kyongju, Korea.The aim of the conference is to discuss and review state-of-the art technology in welding and joining. Attendance is open to any interested parties.

Abstracts are sought for papers to address, but not limited to, the topics below. Metallurgy: phase transformation, weld cracking, property composition, arc physics, weld fracture; high energy processes: laser material processing, electron beam welding, plasma arc welding, microjoining; low-temperature joining: soldering, brazing, adhesive bonding, pressure welding; welding education; automation: sensing and control, welding robotics, monitoring and measurement; design: residual stress and distortion, weldability, modeling and simulation; welding processes: arc welding, resistance welding, special welding processes; welding fabrication: shipbuilding, auto manufacturing, repair welding, special problems.

Abstracts should be no more than 500 words, prepared in Microsoft Word 97 or newer format, and are due by February 15. The abstract should include titles and names of all authors, company affiliation, full mailing address, fax number, e-mail address, and text in English. It can be sent by e-mail, fax or air mail to Program Committee, IWC-Korea 2002, Yusong, P.O. Box 104, Taejon, 305-710 Korea; FAX: +82-42-828-6513; e-mail: koweld@kws.or.kr.